

This item is the archived peer-reviewed author-version of:

The emissions of nitrous oxide and methane from natural soil temperature gradients in a volcanic area in southwest Iceland

Reference:

Maljanen Marja, Yli-Mojjala Heli, Biasi Christina, Leblans Niki, de Boeck Hans, Bjarnadóttir Brynhildur, Sigurdsson Bjarni D.- The emissions of nitrous oxide and methane from natural soil temperature gradients in a volcanic area in southwest Iceland
Soil biology and biochemistry - ISSN 0038-0717 - 109(2017), p. 70-80
Full text (Publisher's DOI): <https://doi.org/10.1016/J.SOILBIO.2017.01.021>
To cite this reference: <https://hdl.handle.net/10067/1406880151162165141>

1 **The emissions of nitrous oxide and methane from natural soil temperature gradients in**
2 **a volcanic area in southwest Iceland**

3

4 Marja Maljanen^{1*}, Heli Yli-Moijala¹, Christina Biasi¹, Niki I. W. Leblans^{2,4}, Hans J. De
5 Boeck², Brynhildur Bjarnadóttir³, Bjarni D. Sigurdsson⁴

6

7 1) University of Eastern Finland, Department of Environmental and Biological Sciences,
8 P.O.Box 1627, Finland (marja.maljanen@uef.fi, christina.biasi@uef.fi)

9 2) Centre of Excellence PLECO (Plant and Vegetation Ecology), Department of
10 Biology, Universiteit Antwerpen (Campus Drie Eiken), Universiteitsplein 1, B-2610
11 Wilrijk, Belgium (niki.leblans@uantwerpen.be, hans.deboeck@uantwerpen.be)

12 3) University of Akureyri, 600 Akureyri, Iceland (brynhildurb@unak.is)

13 4) Agricultural University of Iceland, Keldnaholt, 112 Reykjavik, Iceland
14 (bjarni@lbhi.is)

15

16 *corresponding author (email: marja.maljanen@uef.fi)

17

18

19

20 **Key words:** greenhouse gas, andosol, warming, geothermal, carbon, nitrogen

21 Abstract

22 Nitrous oxide (N₂O) and methane (CH₄) emissions were measured along three natural
23 geothermal soil temperature (T_s) gradients in freely drained upland soils in a volcanic area in
24 Iceland. Two of the T_s gradients (underneath a grassland (GN) and a forest site (FN),
25 respectively) were recently formed (in May 2008) and thus subjected to relatively short-term
26 warming. The third T_s gradient, underneath another grassland site (GO), had been subjected
27 to long-term soil warming (over at least 45 years). The N₂O and CH₄ emissions were
28 measured using the static chamber method. In addition, subsurface soil gas concentrations (5-
29 20 cm) were studied. N₂O emissions from GN were slightly higher than those from GO in the
30 temperature elevation range up to +5 °C, while CH₄ uptake rates were similar. Under
31 moderate soil warming (< +5 °C) there were no significant increases in gas flux rates within
32 any of the sites, but when soil warming exceeded +20 °C, both N₂O and CH₄ emissions
33 increased significantly at all sites. While net uptake of CH₄ (up to -0.15 mg CH₄ m⁻² h⁻¹) and
34 occasional N₂O uptake (up to -12 µg N₂O m⁻² h⁻¹) were measured in the unwarmed plots at all
35 sites, net emissions were only measured from the warmest plots (up to 2600 µg N₂O m⁻² h⁻¹
36 and up to 1.3 mg CH₄ m⁻² h⁻¹). The subsurface soil N₂O concentrations increased with soil
37 warming, indicating enhanced N-turnover. Subsurface soil CH₄ concentrations initially
38 decreased under moderate soil warming (up to +5 °C), but above that threshold they also
39 increased significantly. A portion of the N₂O and CH₄ emitted from the warmest plots may,
40 however, be geothermally derived, this should be further confirmed with isotope studies. In
41 conclusion, our research suggests that moderate increases in soil temperature (up to +5 °C)
42 may not significantly increase N₂O and CH₄ emissions at these upland soils, both in the short
43 and longer term. However, warming trends exceeding +5 °C as predicted for 2100 in
44 pessimistic scenarios may cause increased trace gas emissions and thus significant positive
45 feedbacks to climate change.

46

47 **1. Introduction**

48

49 Nitrous oxide (N₂O) and methane (CH₄) are important greenhouse gases (GHGs). With a
50 100-year time horizon, the global warming potential (GWP) of N₂O is 265 times that of
51 carbon dioxide (CO₂) (IPCC, 2014). N₂O is mainly produced in soils as a consequence of of
52 two microbial activities; aerobic nitrification and anaerobic denitrification (Priemé and
53 Christensen, 2001). The processes forming N₂O as an intermediate product are controlled by
54 several factors such as temperature, moisture, pH and N-availability (Barnard et al., 2005;
55 Brown et al., 2012). This implies that the emissions of N₂O are sensitive to changing
56 environmental conditions. Upland forest soils in the Nordic countries are usually negligible
57 sources of N₂O, whereas N-fertilized agricultural soils and drained peat soils are major
58 sources (Maljanen et al., 2010a).

59

60 Methane has 28 times the GWP of CO₂ over a 100-year time horizon (IPCC, 2014) and is
61 formed in soils by anaerobic methanogenesis (Le Mer and Roger 2001; Serrano-Silva et al.,
62 2014). The production of CH₄ is primarily controlled by oxygen content, but is additionally
63 controlled by soil temperature, pH, moisture and salinity (Le Mer and Roger 2001; Serrano-
64 Silva et al., 2014). Methane that is produced in deeper soils layers can be transported to the
65 atmosphere via ebullition through wet soils, via diffusion, or via the aerenchyma of vascular
66 plants (Marushchak et al., 2016; Serrano-Silva et al., 2014). Methane can be oxidized in the
67 soil by methanotrophic microbes, both under aerobic and anaerobic conditions (Knittel and
68 Boetius, 2009). The optimum conditions for this process include neutral soil pH, a soil
69 temperature of ~25 °C and low salinity (Serrano-Silva et al., 2014). As a consequence, the
70 CH₄ efflux from the soil is the net result of both methane production and methane oxidation.

71 As both processes are controlled by several environmental factors, any change therein can
72 affect this efflux (Le Mer and Roger, 2001). Upland mineral soils are usually small sinks for
73 atmospheric CH₄, whereas waterlogged wetlands are the major sources of CH₄ at northern
74 latitudes (Maljanen et al., 2010a).

75

76 To study the effects of climate change on N₂O and CH₄ fluxes, warming experiments are
77 often employed. However, short-term manipulative warming treatments can be impacted by
78 several confounding factors and can be considered as over-simplistic (De Boeck et al., 2015).
79 Natural temperature gradients (e.g. thermal gradients as a result of geothermal activity) on the
80 other hand offer a number of benefits that makes them suitable “field laboratories” for
81 research on GHG responses to soil warming (Kayler et al., 2015; O’Gorman et al., 2014).
82 Geothermal activity can remain stable for many years, making it possible to investigate long-
83 term warming effects, but major tectonic events can also create new hotspots, exposing
84 previously unwarmed ecosystems to higher temperatures and enabling studies of recent
85 (short-term) temperature responses (O’Gorman et al., 2014).

86

87 Both types of natural soil temperature gradients can be found in the Hellisheiði geothermal
88 systems in southwest Iceland. In May 2008, a major earthquake in southern Iceland affected
89 the geothermal systems close to its epicenter (Halldorsson and Sigbjörnsson, 2009). A part of
90 this geothermal system moved from its previous location to a new and previously unwarmed
91 area, creating a natural soil warming experiment. This offers a unique opportunity to study
92 how various ecosystem processes, including N₂O and CH₄ dynamics, are affected by short-
93 term temperature changes. Other geothermal systems in the area were not affected by the
94 earthquake, providing natural soil temperature gradients that can be used to study long-term
95 soil temperature effects on N₂O and CH₄ dynamics.

96

97 The “ForHot“ research network was established in 2012 to bring European scientists together
98 to study how changes in soil temperature affect various ecosystem processes in both natural
99 grasslands and a planted 45-year old Sitka spruce forest in southern Iceland. The large range
100 in temperature elevations at the ForHot sites offers both conditions similar to the predicted
101 climate change during the next century as well as more extreme temperatures that can yield
102 new insights into stress physiology (Kayler et al., 2015; O’Gorman et al., 2014).

103

104 The major aim of this study within the ForHot project was to investigate changes in N₂O and
105 CH₄ flux rates along soil temperature gradients to better predict the impacts of future soil
106 warming on atmospheric impacts of terrestrial ecosystems. Our hypothesis was that a
107 significant increase in soil temperature will accelerate microbial processes and turn these sites
108 from N₂O and CH₄ sinks to sources.

109

110 **2. Methods**

111

112 **2.1 Study site**

113 The ForHot study sites are located in southwest Iceland, in the surroundings of the village
114 Hveragerdi (64.008°N, 21.178°W), on land owned by the Agricultural University of Iceland
115 (Fig. 1). In 2004-2014, the area had a mean annual air temperature of 5.2 °C and a mean
116 annual precipitation of 1431 mm (Icelandic Met Office, IMO). The growing season normally
117 starts in May and ends in late August. The soil type at the study sites is Brown Andosol
118 (Arnalds, 2015), with relatively high pH (5.5-7.0) and large soil water retention capacity
119 (O’Gorman et al., 2014).

120

121 On the 29th of May, 2008, a major earthquake (magnitude 6.3 on the Richter scale) occurred
122 in southwest Iceland (Halldorsson and Sigbjörnsson, 2009), where ca. 70-100 years pass
123 between such large earthquake episodes in this region. The 2008 earthquake caused large
124 structural damages to infrastructures and affected geothermal systems close to its epicenter.
125 One such geothermal system moved from its previous location to a new and previously
126 unwarmed area (Þorbjörnsson et al., 2009), and the new belowground geothermal channels
127 within the bedrock resulted in soil temperature increases in the soil above. The soil
128 temperature elevation measured at 10 cm soil depth reaches $>50^{\circ}\text{C}$ where the channels are
129 closest to the surface (O’Gorman et al., 2014). The recently warmed area is covered by two
130 different ecosystem types: a) a planted 45 year old Sitka spruce (*Picea sitchensis*) forest
131 (Forest New, FN) and b) a natural, unmanaged treeless grassland (Grassland New, GN)
132 dominated by *Festuca* sp., *Agrostis* sp. and moss (Fig. 1).

133

134 The third study site (Grassland Old, GO) is located 2.5 km NW from GN and FN on an older
135 temperature gradient in Grændalur (the ‘green valley’) allowing to study the long-term effects
136 of warming. It is covered by the same grassland type as GN. At the GO site the earliest
137 survey of geothermal hot-spots was made in 1963-1965 (45 years prior to the 2008
138 earthquake) (Kristján Sæmundsson, pers. comm.). In autumn 2008, the locations of the new
139 and old geothermal hot-spots in the area were mapped and published (Þorbjörnsson et al.,
140 2009). This survey was used to select the GO and GN sites for the ForHot study. Further, the
141 existence of some of the hot-spots prior to the 2008 earthquake at GO is also supported by
142 regular field measurements of soil temperature since 2005 in a previous study in Grændalur
143 (Daebeler, 2014). The geothermal activity has most likely been persistent in Grændalur for
144 centuries, however, as according to local knowledge its name is derived from the subarctic
145 grasslands staying green during most of the winter on the warmest hot-spots. The oldest

146 historical document that mentions this place name was published in 1708 (Magnússon and
147 Vídalín, 1918-1921). Additional evidence for persistent geothermal warming at the GO site
148 are geothermal clay layers found at various depths in the soil profile (Leblans, pers.
149 communication). This indicates that over longer time periods, the warming may have
150 fluctuated somewhat, as was observed at other nearby, older hot-spots following the 2008
151 earthquake (Daebeler, 2014).

152

153 **2.2 Chamber measurements**

154 The gas fluxes (N₂O and CH₄) were measured using the static chamber method (e.g.
155 Maljanen et al., 2010b). The flux measurements were made along temperature gradients in
156 FN, GN and GO during years 2012-2014 in several campaigns during the growing season
157 (May-August) and in GN additionally during one winter campaign in February 2015. There
158 were five to six gas flux sampling points on each gradient. The sampling points were
159 covering unwarmed soil temperature (T_s) and elevated T_s, up to ~ +40, +20 and +11 °C in FN,
160 GN and GO respectively. The warming levels measured in 2012 are indicated in Figs. 3-6
161 with site code (FN, GN or GO) and temperature elevation as +x °C. Because the temperatures
162 along the gradient are slightly changing all the time the actual measured temperatures during
163 gas sampling are shown in the box plots in Figs. 3-6. There were two replicate flux chambers
164 in growing season 2012 and in winter 2015 and three in growing seasons 2013-2014 at each
165 sampling point. The metal flux chambers (ø = 26 cm, h = 30 cm) had a hole in the top for a
166 sampling line. Prior to sampling the sharp edge at the bottom of the chamber was twisted 3-5
167 cm into soil and the top was sealed with a rubber septum. A total of four gas samples (30 ml)
168 were collected 5, 10, 20, and 30 min after installing the chamber with a 60 ml syringe
169 (Terumo). Within 12 h, the samples were injected into 12 ml Labco pre-evacuated vials
170 (Labco Exetainer[®]) for gas analysis with a gas chromatograph at University of Eastern

171 Finland (UEF). Soil temperatures were recorded next to the chambers at each sampling
172 location at depths of 3, 5, 10, 15 and 20 cm.

173

174 **2.3 Soil gas sampling**

175 Soil N₂O and CH₄ concentrations were measured at the sampling points simultaneously with
176 the gas flux measurements in June 2014. Gas samples of 20 ml were taken with a stainless
177 steel sampling probe ($\phi = 3$ mm, $l = 30$ cm) at three soil depths; 5, 10 and 20 cm. Samples of
178 N₂O and CH₄ were treated and analysed as described above.

179

180 **2.4 Gas concentration analysis**

181 Concentrations of N₂O and CH₄ were determined with a gas chromatograph (Agilent 6890N,
182 Agilent Technologies, USA), equipped with an autosampler (Gilson, USA) an electron
183 capture (ECD), and flame ionization detectors (FID). Compressed air, containing 0.836 $\mu\text{l l}^{-1}$
184 of N₂O, and 2.02 $\mu\text{l l}^{-1}$ of CH₄, was used for daily calibration. The gas flux rates were
185 calculated from the linear increase or decrease in the gas concentration with time in the
186 headspace of the chamber. If there were any indications of failure in the gas sampling or gas
187 analysis, the results were excluded from the calculations.

188

189 **2.5 Soil analysis**

190 Soil samples (sampling depths 0-5 cm and 5-10 cm) were collected from all sites in June
191 2014 and transported to UEF for analysis. Soil pH and electric conductivity (EC) were
192 measured from soil/water slurry (15 ml soil: 50 ml milliQ-H₂O) from homogenized and
193 pooled samples. Soil nitrate (NO₃⁻), nitrite (NO₂⁻), chloride (Cl⁻), sulfate (SO₄²⁻), ammonium
194 (NH₄⁺) and dissolved organic carbon (DOC) concentrations were measured from soil
195 extracts. For anion analysis, 15 ml soil and 50 ml H₂O were shaken at 175 rpm for one hour,

196 filtered, and analyzed with an ion chromatograph (DX 120, Dionex Corporation, USA). DOC
197 concentrations were measured from H₂O-extracts with a TOC analyzer (TOC/TNb Analyzer
198 Multi N/C 2100S, Analytik Jena AG). To extract NH₄⁺, 15 ml soil and 50 ml 1M KCl were
199 used. NH₄⁺ was analyzed with a spectrophotometer (Ultrospec 3000 Pro, Biochrom, UK)
200 from the filtered KCl extracts using the method of Fawcett and Scott (1960). Gravimetric soil
201 moisture was determined by drying the soil for 24 h at 105 °C. Organic matter (OM)
202 concentration was determined by loss on ignition at 550 °C. Soil C and N contents were
203 determined with an EA-analyzer (Flash EA 1112 Series, Thermo Electron Corporation,
204 USA).

205

206 **2.6 Statistical analyses**

207 Because the flux data was not normally distributed even after log-transformations the
208 correlations between the gas flux rates and T_s were tested with non-parametric Spearman
209 rank correlation tests. For the correlations between other soil variables, Pearson correlation
210 tests were used. The differences in the gas flux rates were tested with Mann-Whitney U-test
211 (IBM SPSS statistics 19).

212

213 **3. Results**

214

215 **3.1 Soil temperature**

216 Across the summer and autumn measurement campaigns, the mean T_s at 10 cm depth in the
217 unwarmed plots was 8.3, 8.7 and 8.4 °C in FN, GN and GO. T_s gradually increased along the
218 sampling transect up to 50.4, 28.4 and 18.0 °C, in FN, GN and GO respectively (Fig. 2; Figs.
219 3-5.). During the winter campaign at the GN site in February 2015 (Fig. 6), T_s were lower
220 (ranging from -0.5 to 12.4 °C) than during the growing season (Fig. 4).

221

222 3.2 Soil properties

223 The measured soil properties are presented in Table S1. Soil pH increased with increasing
224 temperature ($r = 0.805$, $p = 0.001$; $r = 0.811$, $p = 0.002$) in FN and GN, respectively (Fig. 2).
225 The pH of unwarmed soils varied from 5.2 in FN to 5.7 in GO, and up to 7.3 in GN (Fig. 2).
226 Soil OM concentrations at depths of 5-10 cm decreased with T_s see Fig 2. ($r = -0.693$, $p =$
227 0.038 ; $r = -0.731$, $p = 0.039$; $r = -0.841$, $p = 0.009$ for FN, GN and GO respectively). Soil C
228 and N concentrations decreased with increasing T_s , but this decrease was only significant in
229 FN ($r = -0.819$, $p = 0.007$ and $r = -0.750$, $p = 0.020$) and GN ($r = -0.749$, $p = 0.320$ and $r = -$
230 0.737 , $p = 0.370$). However, soil gravimetric moisture, EC, NO_3^- , NH_4^+ , DOC, SO_4^{2-} or Cl^-
231 content did not correlate with T_s at any of the sites (Table S1). Soil nitrite (NO_2^-)
232 concentrations were lower than the detection limit of $0.01 \mu\text{g g}^{-1}$ soil in all samples.

233

234 3.3 Gas flux rates

235 With a moderate T_s increase (up to $+5^\circ\text{C}$), no statistically significant increase of N_2O or CH_4
236 flux rates were observed at any of the sites. However, beyond the $+5^\circ\text{C}$ warming threshold,
237 both N_2O and CH_4 emissions increased (Figs. 3-5). Nitrous oxide emissions from the short-
238 term warmed grassland (GN) were slightly higher than those from the long-term warmed
239 grassland (GO), associated with temperature increase of $\leq +5^\circ\text{C}$ but CH_4 uptake rates were
240 similar. While a net uptake of CH_4 (up to $-0.15 \text{ mg CH}_4 \text{ m}^{-2} \text{ h}^{-1}$) and occasionally also N_2O
241 uptake (up to $-12 \mu\text{g N}_2\text{O m}^{-2} \text{ h}^{-1}$) were measured in the unwarmed plots, net emissions were
242 measured at all the warmest plots. Because T_s in the sampling plots varied with time (due to
243 variation in ambient air temperature and minor fluctuations in the geothermal warming) the
244 actual temperatures during sampling are shown in Figs. 3-6. The measured N_2O emissions
245 from plots with the most extreme T_s increase (Site FN $\sim +40^\circ\text{C}$ and GN $\sim +20^\circ\text{C}$) were two

246 magnitudes higher (maximum up to $2600 \mu\text{g N}_2\text{O m}^{-2} \text{h}^{-1}$) compared to the unwarmed control
247 plots (less than $20 \mu\text{g N}_2\text{O m}^{-2} \text{h}^{-1}$) (Table 1, Figs. 3, 4). At the GO site, the highest N_2O
248 emissions were also measured at the warmest plot, which was on average $\sim +11 \text{ }^\circ\text{C}$ warmer
249 than the unwarmed soils (Fig. 5). However, at all other sampling points at the GO site, N_2O
250 emissions were similar along the gradient. The CH_4 fluxes only correlated significantly with
251 increasing T_s at the GO site (Table 1).

252

253 The winter N_2O emission rates at the GN plots did not differ significantly from those during
254 the growing season. However, the winter CH_4 fluxes were less often negative (uptake) than
255 during the growing season ($p < 0.001$; Mann-Whitney U-test). The winter N_2O emissions
256 increased with increasing T_s ($r = 0.488$, $p < 0.001$, Fig. 6), while the winter CH_4 fluxes did
257 not correlate with T_s .

258

259 **3.4 Gas concentrations in soil**

260 The soil N_2O and CH_4 concentrations, sampled with a metal probe from 5, 10 and 20 cm soil
261 depth varied significantly between plots and depths (Fig. 7). Soil N_2O concentrations
262 increased with depth, up to $100 \mu\text{l l}^{-1}$, at GN and FN sites. At GO site the N_2O concentrations
263 were similar, less than $1 \mu\text{l l}^{-1}$, in all plots and all depths except slightly higher in the warmest
264 ($+11 \text{ }^\circ\text{C}$) plot (Fig. 7). The CH_4 concentrations also increased with depth in the warmest
265 plots, but the opposite was true for the unwarmed control plots, where soil CH_4 concentration
266 was the lowest at 20 cm depth (Fig. 7).

267

268 4. Discussion

269

270 In this study soil temperature increases of less than 5 °C did not significantly affect soil
271 emissions of N₂O and CH₄. The N₂O emissions from the unwarmed forest soil were relatively
272 low (mean 2.5 µg m⁻² h⁻¹), and were in the range of previous reports for boreal upland forest
273 soils in the Nordic countries (e.g. Maljanen et al., 2010a; 2010b). The N₂O emissions from
274 the unwarmed grassland soil were also low (mean emissions from GN were 3.9 µg m⁻² h⁻¹ and
275 from GO 2.2 µg m⁻² h⁻¹). Only in the plots with extreme soil temperature elevations (up to
276 +53 °C), N₂O emissions were significantly enhanced (up to 2600 µg m⁻² h⁻¹). The magnitude
277 was higher than earlier reported from drained peat soils, which are considered to be the hot
278 spots for N₂O emissions in the Nordic countries (Maljanen et al., 2010a). The increase in N₂O
279 emissions at the warmest plots may be related to higher nitrogen mineralization and
280 nitrification rates, which are frequently found in soils subjected to warming treatment in the
281 North (e.g. Biasi et al., 2008). However, N₂O may be at least partly geothermally derived as
282 reported by Klusman et al. (2000) from geothermal fields in the USA and discussed further
283 below.

284

285 Unwarmed forest and grassland soils were small sinks for CH₄ (mean -0.4 mg m⁻² h⁻¹), with
286 only the warmest plots producing net CH₄ emissions (up to 1.33 mg m⁻² h⁻¹). Elevated
287 temperatures (in the range of +5 to +25 °C) have been shown to decrease CH₄ uptake in soils
288 (Dijkstra et al., 2011). In our study, moderate warming (up to +5 °C) led to a slight increase in
289 CH₄ uptake, but when temperature increased by more than 5 °C, the soils turned into net CH₄
290 sources. Our data suggest a seasonal trend in CH₄ fluxes. In summer, the cooler plots (below
291 +5 °C) were primarily CH₄ sinks, while the warmer plots were CH₄ sources. In winter, on the
292 contrary, all CH₄ fluxes at GN site were close to zero as a consequence of the low soil

293 temperatures. Methane can also be produced in both biological and geothermal processes
294 (Tassi et al., 2012). Especially the very high CH₄ emissions from the warmest plots are
295 difficult to explain from biological sources only. Upland mineral soils with low organic
296 matter and water content are usually sinks for atmospheric CH₄ as a result of methane
297 oxidation in the oxic top soil and such high emissions are uncommon (Le Mer and Roger
298 2001; Megonigal and Guenther 2008).

299

300 There is some evidence that supports the assumption that the source of the high N₂O and CH₄
301 emissions are non-biological, from a geothermal source. Rey (2015) reported that in
302 geothermal areas the geological CO₂ can play an important role in the soil CO₂ emissions,
303 which has been observed also in nearby geothermal areas in Iceland (Fridriksson et al., 2006).
304 This could also be true for N₂O (Klusman et al., 2000). The concentration of mineral N
305 (NH₄⁺ or NO₃⁻) did not increase with soil temperature (Supplementary Table 1) or correlate
306 with N₂O emissions. However, further studies are needed to confirm the hypothesis that non-
307 biological sources contribute to the overall N₂O and CH₄ release in geothermal areas,
308 particularly isotope studies of both GHGs in soil profile and surface emissions. The isotope
309 signal of N₂O from geothermal sources has, to the best of our knowledge, not been
310 characterized so far, but it is likely that it differs significantly from biological or atmospheric
311 sources (as found for N₂ from hydrothermal fluids; Caliro et al., 2015). Similarly, CH₄ from
312 geothermal reservoirs exhibits a different δ¹³C values than biologically produced CH₄ (it is
313 more enriched in ¹³C; Klusman et al., 2000) which would aid the source identification of
314 CH₄. As mentioned already above, we hypothesize that geothermal CH₄, reported by e.g.
315 Etiope and Klusman (2002) and Klusman et al. (2000), may also be present in the ForHot
316 research area since such high CH₄ emissions at the warmest plots are difficult to explain from
317 upland mineral soils. The very high concentrations of CH₄ in the deeper soil profiles indicates

318 there must be a significant source for CH₄. High CH₄ concentrations, not associated with any
319 geothermal origin, have not been found in upland mineral soils in contrast to wetland soils
320 (LeMer and Roger 2001).

321

322 These geothermally active sites can act as local hot spots for N₂O or CH₄ emissions
323 (Klusman et al., 2000). While N₂O emissions from such sites are not well documented, the
324 global geothermal emissions of CH₄ are estimated in the range of 3-7 Mt year⁻¹ (Etiope and
325 Klusman, 2002; Etiope et al., 2008; Lacroix, 1993). Etiope (2009) reported that even one
326 third of Europe's methane emissions can be geological origin. Data on geothermal emissions
327 of N₂O are lacking, but would be important for better estimating the global N₂O budget.

328

329 However, there can be also biological factors explaining partly the change in GHG flux rates
330 with increasing temperature. Soil organic matter content as well as C content decreased with
331 increasing soil temperature in the FN and GN site, indicating that organic matter is already
332 more decomposed in the warmer plots during the first six years after the formation of these
333 gradients. The availability of organic matter can positively affect the CH₄ production as well
334 as N₂O production in the soil (Harrison-Kirk et al., 2013; Le Mer and Roger, 2001; Maljanen
335 et al., 2009). On the other hand, in the GO site, the increase in soil temperature was smaller
336 than in the other sites and we did not see any dramatic changes either in the flux rates or in
337 the soil gas concentrations. However, there was a clear decrease in soil OM, C and N content
338 with increasing soil temperature, which could indicate that most of the C and N had already
339 been lost from the warmest plots, possibly limiting the microbiological production of CH₄
340 and N₂O.

341

342 The clear increase in soil pH with increasing soil temperature could favor denitrification.
343 Nitrification and denitrification activities are favored by neutral soil pH (e.g. Brenzinger et
344 al., 2015), but at the same time N₂O reductase is favored by high pH. Therefore, N₂O should
345 be more efficiently reduced to N₂ at higher pH. The activity of methanogens (CH₄
346 production) and methanotrophs (CH₄ oxidation) is favored also by neutral soil pH (Le Mer
347 and Roger, 2001). In this study, the net CH₄ production was increasing more than CH₄
348 oxidation, as it increased with pH.

349
350 We did not observe any significant changes in the N₂O or CH₄ flux rates associated with
351 moderate soil temperature increases (< 5 °C). The expected increase in soil temperature as a
352 result of global warming for the subarctic sites ranges from 2.6 to 8.5 °C by the end of this
353 century (IPCC, 2014). If the most pessimistic scenario would come true, more N₂O and CH₄
354 emissions from northern soils can be expected, if the sources of these two trace gases
355 investigated here are from biological origin. When soil temperature increased by more than
356 10 °C, the flux rates increased significantly at the short-term warmed FN and GN sites, but
357 not at the long-term warmed GO site, which could be the result of less C and N available at
358 the long term warmed sites. In any case, we can conclude that a moderate increase (< 5 °C) in
359 soil temperature with climate change would not significantly increase N₂O or CH₄ emissions
360 from the studied soils. In this study, we cannot separate the role of microbial activity from
361 geothermal causes in explaining the dramatic increase in N₂O or CH₄ flux rates from the
362 warmest soils, but we speculate that geothermal sources play a role. By employing stable
363 isotope analysis of CH₄ and N₂O, we could further examine the mechanisms that underlie
364 changes in flux dynamics. By doing so, the role of geothermal and biological processes can
365 be investigated in more detail which is needed in order to conclusively interpret the results
366 from studies on thermal gradients in geothermal areas, in predicting climate change impacts.

367 Better estimates on geothermal sources of N₂O and CH₄ would be needed in order to better
368 constrain the global budget of these trace gases.

369

370 **Acknowledgements**

371 Hanne Säppi, Tatiana Trubnikova and Joonas Maljanen are thanked for assisting in the
372 laboratory. Sigmundur H. Brink made the overview map. This work contributes to the COST
373 ES1308 ClimMani, the Nordic CAR-ES and the ForHot (www.forhot.is) network projects.
374 The Icelandic-Finnish Cultural Foundation is thanked for travel grants. Further, this research
375 was supported by the Research Foundation – Flanders (FWO aspirant grant to NL). We also
376 want to acknowledge the staff at the Reykir campus of Agricultural University of Iceland for
377 great logistic support. The study was further supported by strategic funding of the University
378 of Eastern Finland (project FiWER granted to CB).

379

380 **References**

381 Arnalds, O. 2015. The Soils of Iceland. Springer Netherlands.

382

383 Barnard, R., Leadley, P.W., Hungate, B.A. 2005. Global change, nitrification, and
384 denitrification: A review. *Global Biogeochemical Cycles* 19, doi: 10/1029/2004GB002282,
385 2005.

386

387 Biasi, C., Meyer, H., Rusalimova, O., Hämmerle, R., Kaiser, C., Baranyi, C., Daims, H.,
388 Lashchinsky, N., Barsukov, P., Richter, A. 2008. Initial effects of experimental warming on
389 carbon exchange rates, plant growth and microbial dynamics of a lichen-rich dwarf shrub
390 tundra in Siberia. *Plant and Soil* 307, 191–205.

391

- 392 Brenzinger, K., Dörsch, P., Braker, G. 2015. pH-driven shifts in overall and transcriptionally
393 active denitrifiers control gaseous product stoichiometry in growth experiments with
394 extracted bacteria from soil. *Frontiers in Microbiology* 6
395 <http://dx.doi.org/10.3389/fmicb.2015.00961>
396
- 397 Brown, J.R., Blankinship, J.C., Niboyet, A., van Groenigen, K.J., Dijkstra, P., Le Roux, X.,
398 Leadley, P.W., Hungate, B.A. 2012. Effects of multiple global change treatments on soil N₂O
399 fluxes. *Biogeochemistry* 109, 85-100.
400
- 401 Caliro, S., Viveiros, F., Chiodini, G., Ferreira, T. 2015. Gas geochemistry of hydrothermal
402 fluids of the S. Miguel and Terceira Islands, Azores. *Geochimica et Cosmochimica Acta* 168,
403 43-57.
404
- 405 Daebeler, A. 2014. Archaeal ammonia oxidation in volcanic grassland soils of Iceland:
406 Effects of temperature and N availability on processes and organisms. (PhD thesis), Utrecht
407 University, Utrecht, the Netherlands, 164 pp.
408
- 409 De Boeck, H.J., Vicca, S., Roy, J., Nijs, I., Milcu, A., Kreyling, J., Jentsch, A., Chabbi, A.,
410 Campioli, M., Callaghan, T., Beierkuhnlein, C., Beier, C. 2015. Global change experiments:
411 challenges and opportunities. *Bioscience* 65, 922-931. doi:10.1093/biosci/biv099
412
- 413 Dijkstra, F.A., Morgan, J.A., von Fisher, J.C., Follet, R.F. 2011. Elevated CO₂ and warming
414 effects on CH₄ uptake in a semiarid grassland below optimum soil moisture. *Journal of*
415 *Geophysical Research* 116, doi: 10.1029/2010JHG001288.
416

- 417 Etiope, G., Klusman, R.W. 2002. Geologic emissions of methane to the atmosphere.
418 *Chemosphere* 49, 777-789.
419
- 420 Etiope, G., Lassey, K.R., Klusman, R.W., Boschi, E. 2008. Reappraisal of the fossil methane
421 budget and related emission from geologic sources. *Geophysical Research Letters* 35,
422 L09307, doi:10.1029/2008GL033623.
423
- 424 Fawcett, J.K., Scott, J.E. 1960. A Rapid and precise method for the determination of urea.
425 *Journal of Clinical Pathology* 13, 156-159.
426
- 427 Fridriksson, T., Kristjánsson, B. R., Ármannsson, H., Margrétardóttir, E., Ólafsdóttir, S., &
428 Chiodini, G. 2006. CO₂ emissions and heat flow through soil, fumaroles, and steam heated
429 mud pools at the Reykjanes geothermal area, SW Iceland. *Applied Geochemistry*, 21(9),
430 1551-1569. doi:<http://dx.doi.org/10.1016/j.apgeochem.2006.04.006>
431
- 432 Halldorsson, B., Sigbjornsson, R. 2009. The Mw6.3 Ölfus earthquake at 15:45 UTC on 29
433 May 2008 in South Iceland: ICEARRAY strong-motion recordings. *Soil Dynamics and*
434 *Earthquake Engineering* 29, 1073-1083.
435
- 436 Harrison-Kirk, T., Beare, M.H., Meenken, E.D., Condon, L.M. 2013. Soil organic matter
437 and texture affect responses to dry/wet cycles: Effects on carbon dioxide and nitrous oxide
438 emissions. *Soil Biology and Biochemistry* 57, 43-55.
439
- 440 IPCC, 2014. *Climate Change 2014: Synthesis Report. Contribution of Working Groups I, II*
441 *and III to the Fifth Assessment Report of the Intergovernmental Panel on Climate Change*

442 [Core Writing Team, R.K. Pachauri and L.A. Meyer (eds.)]. IPCC, Geneva, Switzerland, 151
443 pp.

444

445 Kayler, Z.E., De Boeck, H.J., Fatichi, S., Grünzweig, J.M., Merbold, L., Beier, C.,
446 McDowell, N., Dukes, J.S. 2015. Experiments to confront the environmental extremes of
447 climate change. *Frontiers in Ecology and the Environment* 13, 219–225. doi:10.1890/140174.

448

449 Klusman, R.W., Moore, J.N., LeRoy, M.P. 2000. Potential for surface gas flux measurements
450 in exploration and surface evaluation of geothermal resources. *Geothermics* 29, 637-670.

451

452 Knittel, K, Boetius, A. 2009. Anaerobic oxidation of methane: progress with an unknown
453 processes. *Annual Review of Microbiology* 63, 311-334.

454

455 Lacroix, A.V. 1993. Unaccounted-for sources of fossil and isotopically-enriched methane and
456 their contribution to the emissions inventory: A Review and Synthesis. *Chemosphere* 26,
457 507-557.

458

459 Le Mer, J., Roger, P. 2001. Production, oxidation, emission and consumption of methane by
460 soils: A review. *European Journal of Soil Biology* 37, 25-50.

461

462 Magnússon, Á., Vídalín, P. 1918-1921. Jarðabók. Annað bindi [The farm register of Iceland.
463 2nd Volume], Copenhagen (Originally published in 1708) (In Icelandic).

464

- 465 Maljanen, M., Virkajärvi, P., Hytönen, J., Öquist, M., Sparrman, T., Martikainen, P.J. 2009.
466 Nitrous oxide production in boreal soils with variable organic matter content at low
467 temperature – snow manipulation experiment. *Biogeosciences* 6, 2461-2473.
468
- 469 Maljanen, M., Óskarsson, H., Sigurdsson, B.D., Guðmundsson, J., Huttunen, J.T.,
470 Martikainen, P.J. 2010a. Greenhouse gas balances of managed peatlands in the Nordic
471 countries – present knowledge and gaps. *Biogeosciences* 7, 2711–2738.
472
- 473 Maljanen, M., Alm, J., Martikainen, P.J., Repo, T. 2010b. Prolongation of soil frost resulting
474 from reduced snow cover increases nitrous oxide emissions from boreal forest soil. *Boreal*
475 *Environment Research* 15, 34-42.
476
- 477 Marushchak, M.E., Friborg, T., Biasi, C., Herbst, M., Johansson, T., Kiepe, I., Liimatainen,
478 M., Lind, S.E., Martikainen, P.J., Virtanen, T., Soegaard, H., Shurpali, N.J. 2016. Methane
479 dynamics in the subarctic tundra: combining stable isotope analyses, plot- and ecosystem-
480 scale flux measurements. *Biogeosciences*, 13, 597–608, 2016.
481
- 482 Megonigal, J.P., Guenther, A.B. 2008. Methane emissions from upland forest soils and
483 vegetation. *Tree Physiology* 28, 491-498.
484
- 485 O’Gorman, E., Benstead, J. P., Cross, W. F., Friberg, N., Hood, J. M., Johnson, P. W.,
486 Sigurdsson, B. D., Woodward, G. 2014. Climate change and geothermal ecosystems: natural
487 laboratories, sentinel systems, and future refugia. *Global Change Biology* 20, 3291–3299.
488

489 Priemé, A., Christensen S. 2001. Natural perturbations, drying-wetting and freezing-thawing
490 cycles, and the emission of nitrous oxide, carbon dioxide and methane from farmed organic
491 soils. *Soil Biology and Biochemistry* 33, 2083-2091.

492

493 Rey, A. 2015. Mind the gap: non-biological processes contributing to soil CO₂ efflux. *Global
494 Change Biology* 21, 1752-1761.

495

496 Serrano-Silva, N., Sarria-Guzman, Y., Dendooven, L., Luna-Guido M. 2014. Methanogenesis
497 and Methanotrophy in Soil: A Review. *Pedosphere* 24, 291–307.

498

499 Tassi, F., Fiebig, J., Vaselli, O., Nocentini, M. 2012. Origins of methane discharging from
500 volcanic-hydrothermal, geothermal and cold emissions in Italy. *Chemical Geology* 310–311,
501 36–48.

502

503 Þorbjörnsson, D., Sæmundsson, K., Kristinsson, S.G., Kristjánsson, B.R., Ágústsson, K.

504 2009. Suðurlandsskjálftar 29. maí 2008. Áhrif á grunnvatnsborð, hveravirkni og

505 sprungumyndun [The South Iceland earthquake on 29th of May 2008. Impacts on

506 groundwater levels, activity of geothermal hot-spots and creation of seismic cracks]. *Unnið*

507 fyrir Orkuveitu Reykjavíkur, ÍSOR-2009/028. Iceland Geosurvey, Reykjavik, 42 pp (in

508 Icelandic).

509

510 **Tables**

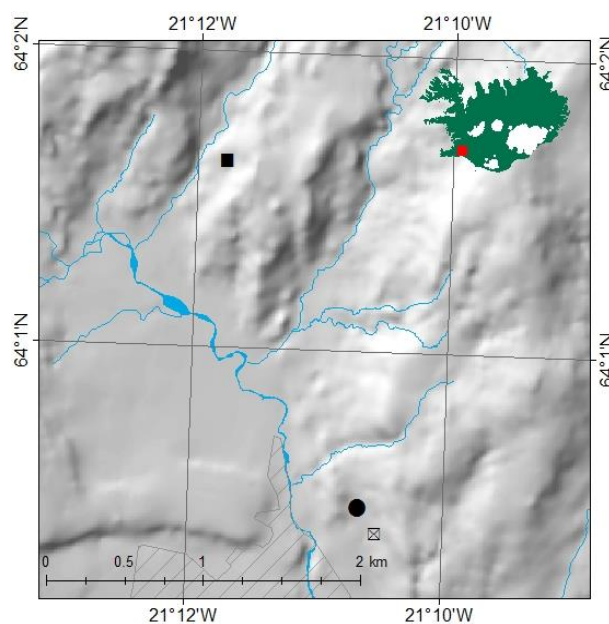
511 **Table 1.** Spearman rank correlation coefficients between soil temperature at 5 and 10 cm
 512 depth and N₂O and CH₄ flux rates during the growing seasons from the temperature gradients
 513 at the forest (FN), the new grassland (GN) and the old grassland (GO) site. ** = p < 0.001, *
 514 = p < 0.05.

Site FN	T ₅	T ₁₀	N ₂ O	CH ₄
T ₁₀	0.996**			
N ₂ O	0.422**	0.411**		
CH ₄	0.411**	0.410**	0.408**	

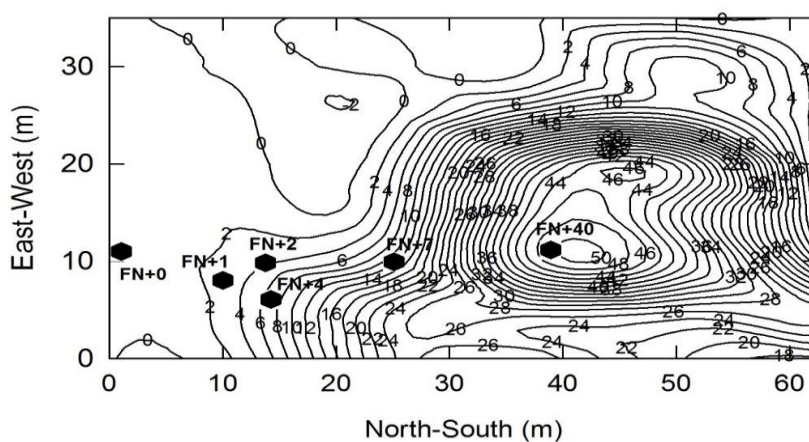
Site GN	T ₅	T ₁₀	N ₂ O	CH ₄
T ₁₀	0.993**			
N ₂ O	0.468**	0.495**		
CH ₄	0.432**	0.439**	0.393**	

Site GO	T ₅	T ₁₀	N ₂ O	CH ₄
T ₁₀	0.996**			
N ₂ O	0.001	0.023		
CH ₄	0.595**	0.598**	0.011	

517

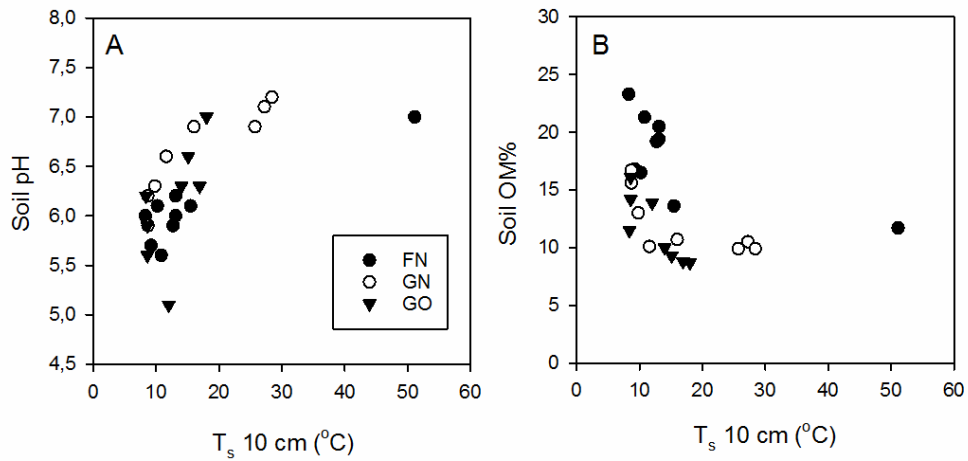
518 **Figures**

519



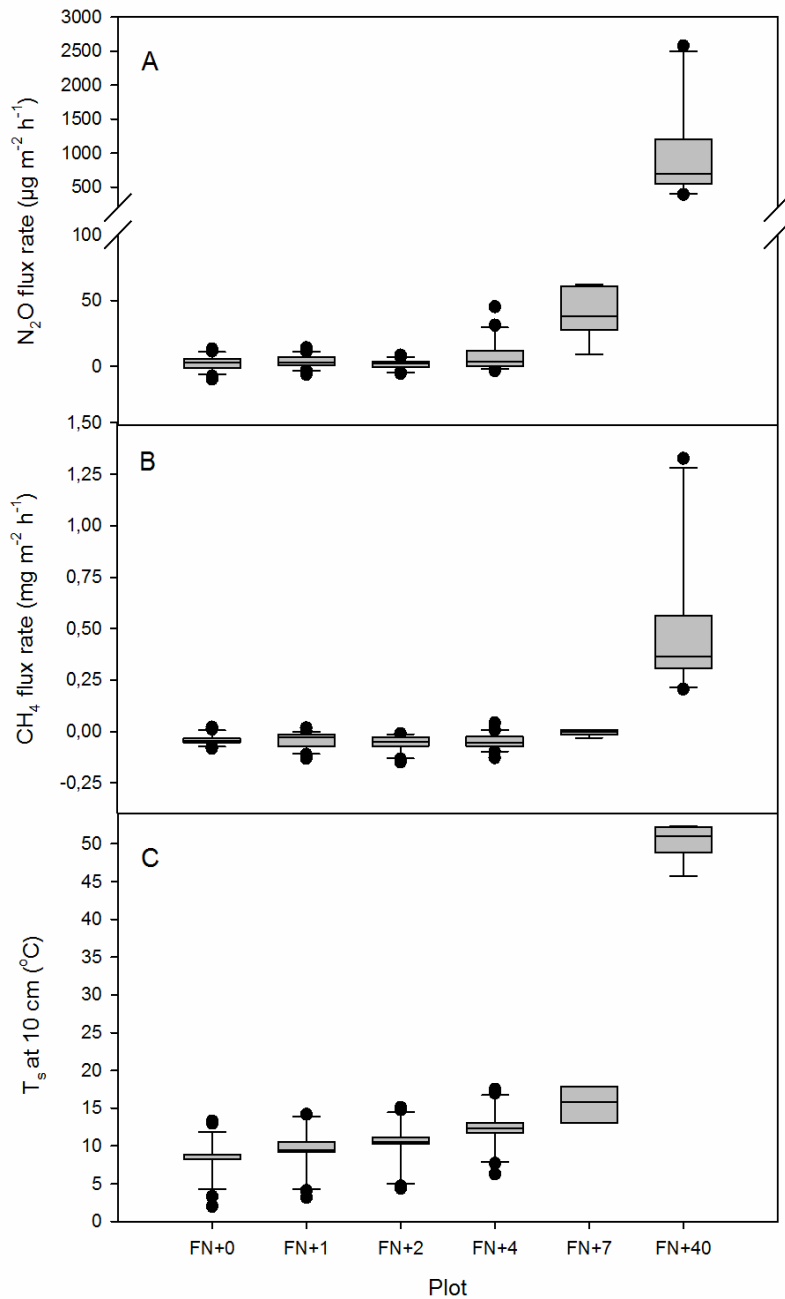
520

521 **Fig. 1.** Location of the three study sites in southern Iceland (upper panel). The circle marks
 522 the recently warmed forest site (FN), the crosshatched square the recently warmed grassland
 523 (GN) and the filled square the grassland with long-term soil warming (GO). The hatched area
 524 represents the village of Hveragerdi. Soil warming isotherms ($^{\circ}\text{C}$) within the FN site in spring
 525 2012 (lower panel), where the natural background soil temperature (T_s) varied by -2 to $+2$ $^{\circ}\text{C}$
 526 in differently shaded parts of the stand and the actual geothermal warming was ca. 2 $^{\circ}\text{C}$ lower
 527 than the isolines indicate. The location of the study plots is also shown, where the measured
 528 geothermal warming at 10 cm depth were determined as 0, +1, +2, +4, +7 and ca. +40 $^{\circ}\text{C}$.



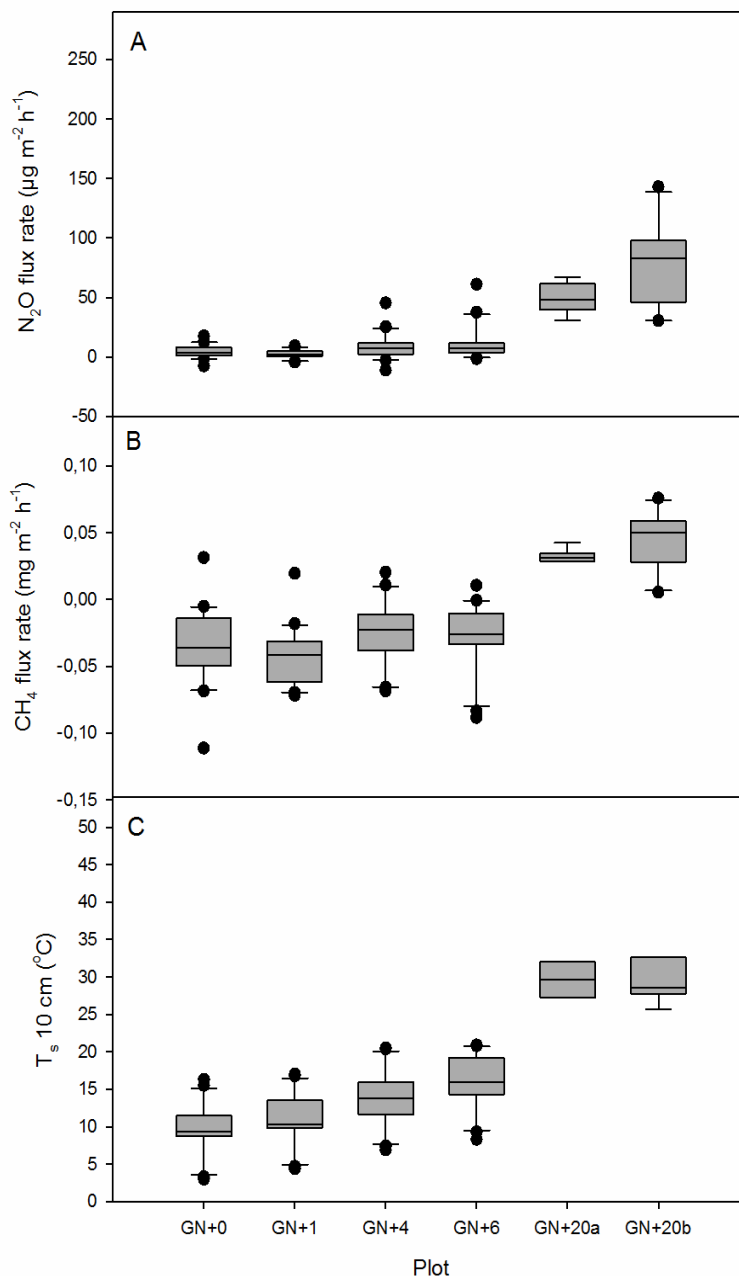
529

530 **Fig. 2.** Soil pH (A) and organic matter (B) concentration (%) at a depth of 5-10 cm, plotted
 531 against soil temperature (T_s) at a depth of 10 cm, measured in June 2014. Black circles
 532 represent the forest site (FN), open circles represent the new grassland site (GN) and triangles
 533 represent the old grassland (GO).



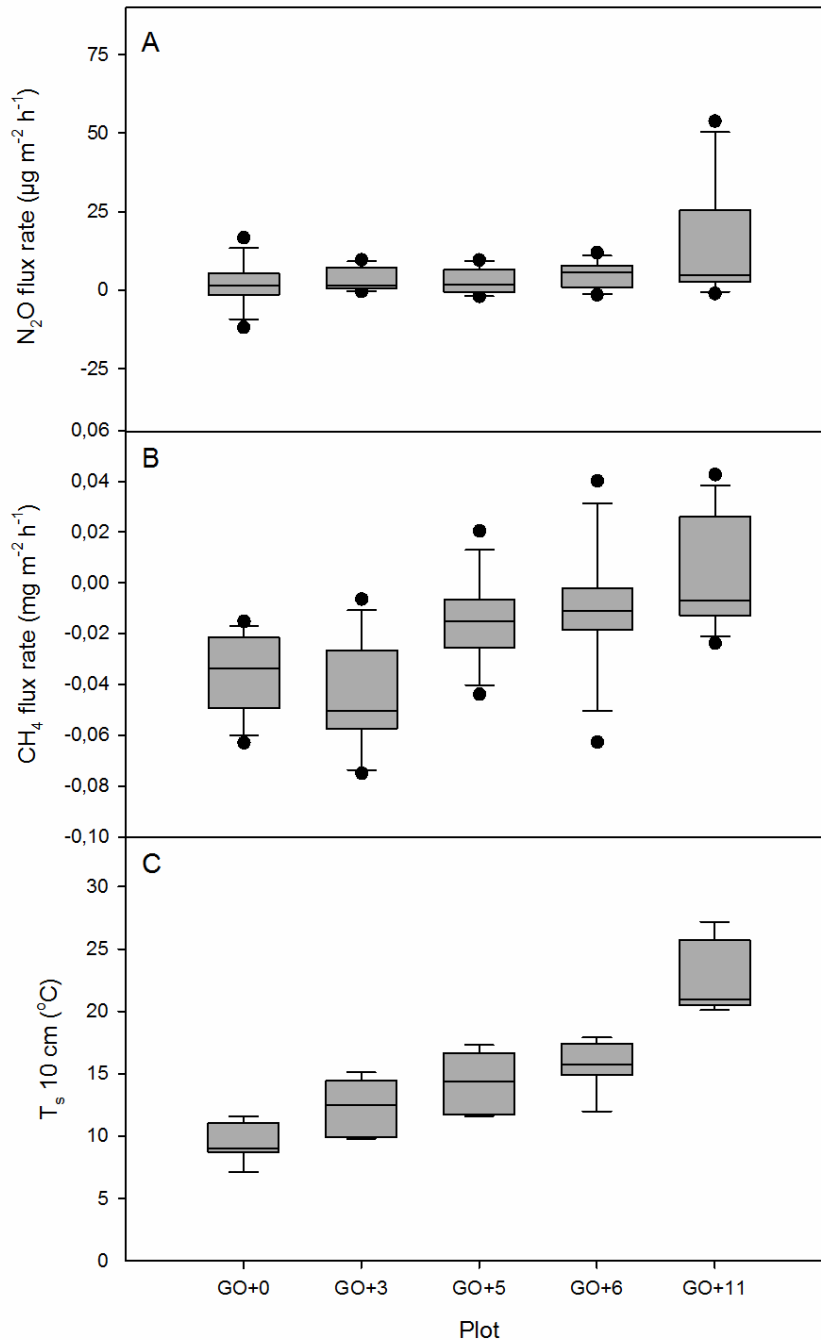
534

535 **Fig. 3.** Flux rates of N_2O (A) and CH_4 (B) and the average soil temperature (T_s) at a depth of
 536 10 cm during sampling at forest (FN) site, measured during the growing seasons of 2012 -
 537 2014. The median, 25th and 75th percentiles are shown in the box with whiskers indicating
 538 variability outside the 25th and 75th percentiles. Plot codes at the x-axis show the average
 539 soil temperature increase ($^{\circ}C$). Plots FN+0 to FN+4 were measured eight times, while plots
 540 FN+7 and FN+40 were measured four times. Each time, two or three replicate chambers were
 541 used (see Methods).



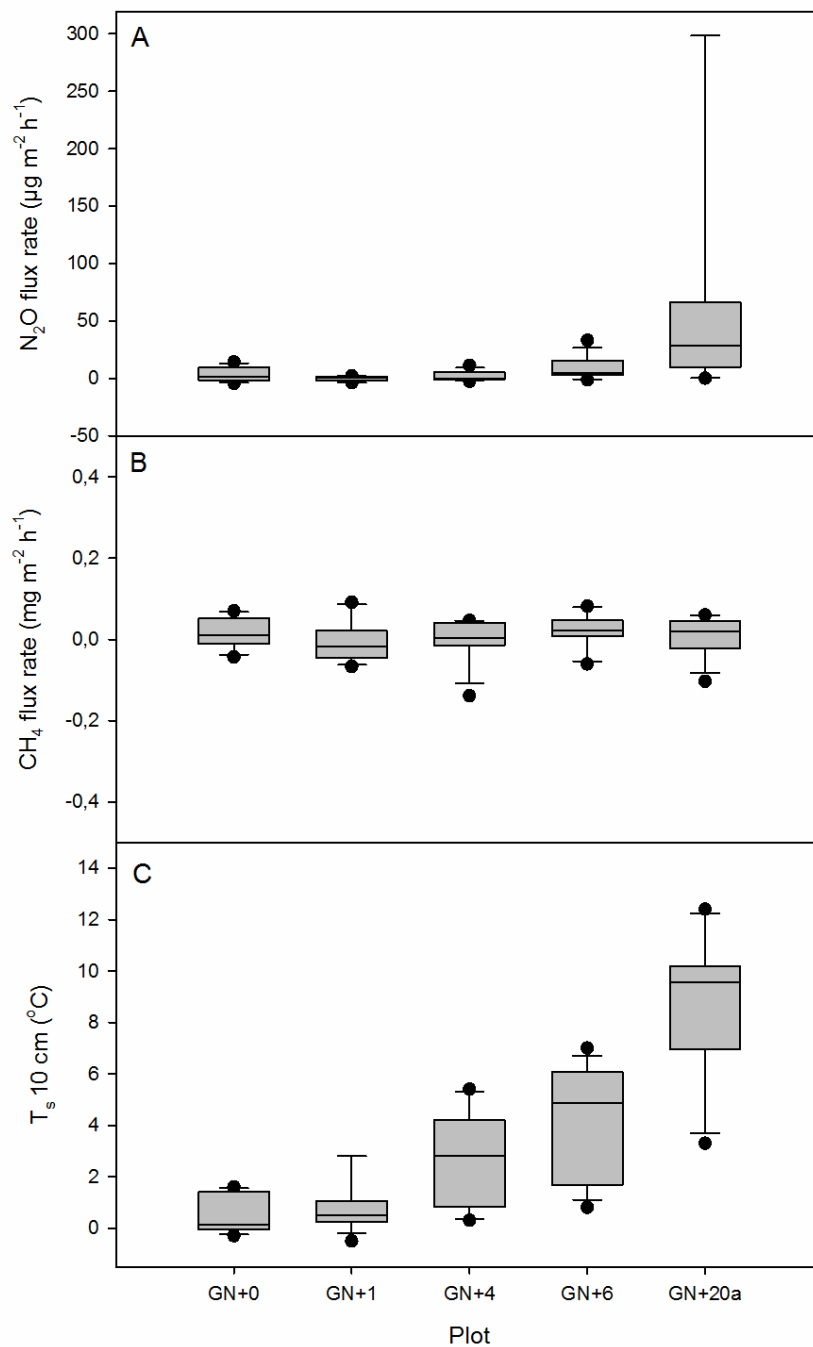
542

543 **Fig. 4.** Flux rates of N₂O (A) and CH₄ (B) and the average soil temperature (T_s) at a depth of
 544 10 cm during sampling at grassland (GN) site, measured during the growing seasons of 2012
 545 - 2014. The median, 25th and 75th percentiles are shown in the box with whiskers indicating
 546 variability outside the 25th and 75th percentiles. Plot codes at the x-axis show the average
 547 soil temperature increase (°C). Plots GN+0 to FN+6 were measured eight times, while plots
 548 GN+20a and GN+20b were measured four times. Each time, two or three replicate chambers
 549 were used.



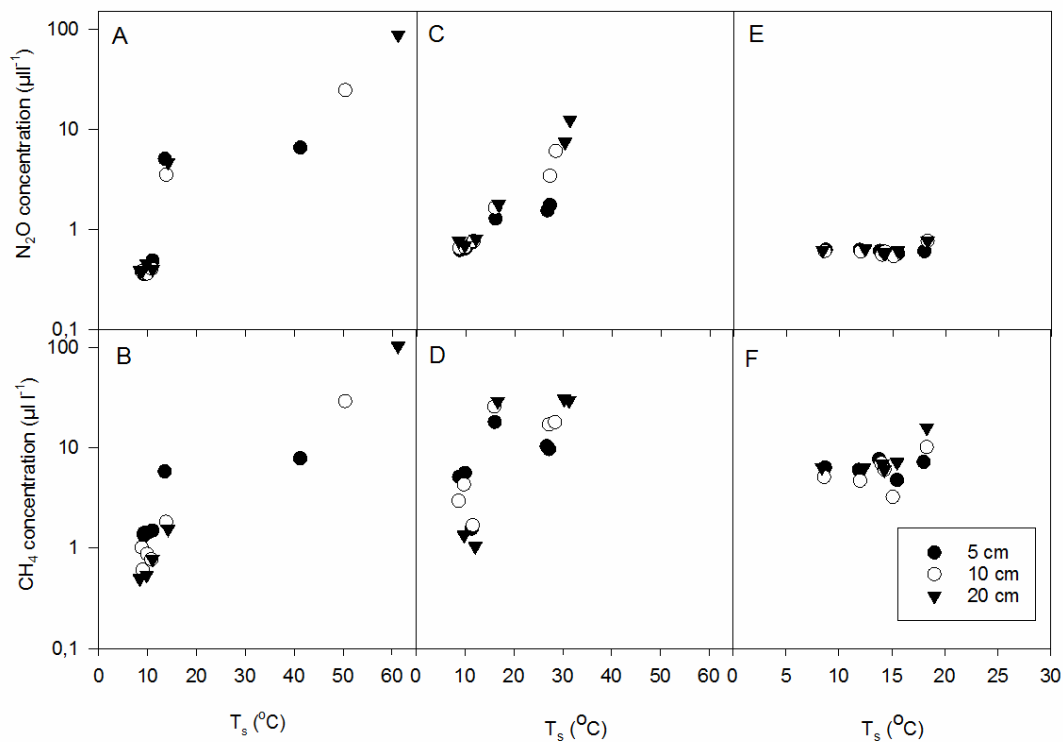
550

551 **Fig. 5.** Flux rates of N₂O (A) and CH₄ (B) and the average soil temperature (T_s, °C) at a
 552 depth of 10 cm during the sampling from the old grassland temperature gradient (GO,
 553 measured during the growing seasons of 2013 and 2014. The median, 25th and 75th
 554 percentiles are shown in the box with whiskers indicating variability outside the 25th and
 555 75th percentiles. Plot codes at the x-axis show the average soil temperature increase (°C).
 556 Each plot was measured five times with two or three replicate chambers.



557

558 **Fig. 6.** Flux rates of N_2O (A) and CH_4 (B) and the average soil temperature (T_s , $^{\circ}\text{C}$) at a
 559 depth of 10 cm during the sampling from the grassland (GN) temperature gradient, measured
 560 in February 2015. The median, 25th and 75th percentiles are shown in the box with whiskers
 561 indicating variability outside the 25th and 75th percentiles. The plot codes are similar as in
 562 Fig. 4 and indicate soil temperature increases during growing the growing season. Each plot
 563 was measured seven times with two replicate chambers.



564

565 **Fig. 7.** N₂O and CH₄ concentrations (μl l⁻¹) measured at 5, 10 and 20 cm soil depth at the FN
 566 site (A, B), the GN site (C, D) and the GO site (E, F), plotted against soil temperature at
 567 sampling depth in June 2014. Note the logarithmic scale on the y-axis.